Macromolecules

ARTICLE

pubs.acs.org/Macromolecules

Radical Grafting of Tetrafluoroethylene and Vinylidene Fluoride Telomers onto Silica Bearing Vinyl Groups

Nelly Durand,[†] Philippe Gaveau,[‡] Gilles Silly,[§] Bruno Améduri,[†,*] and Bernard Boutevin[†]

[†]Ingénierie et Architectures Macromoléculaires, Ecole Nationale Supérieure de Chimie de Montpellier (UMR 5253-CNRS), 8, rue de l'Ecole Normale, 34296 Montpellier Cedex 1, France

[‡]Institut Charles Gerhardt de Montpellier (UMR 5253-CNRS), Université de Montpellier 2, place Eugène Bataillon, 34095 Montpellier Cedex 5, France

[§]Chalcogénures et Verres, Institut Charles Gerhardt (UMR 5253-CNRS), CC1503, Université de Montpellier 2, Place Eugène Bataillon, 34095 Montpellier cedex 5, France

Supporting Information

ABSTRACT: Radical addition of ω-iodofluorinated telomers was used to modify silica (S_{50}) nanoparticles bearing vinyl groups. These iodo terminated derivatives were either commercially available tetrafluoroethylene telomers, $C_nF_{2n+1}I$ with n = 4 or 6, or vinylidene fluoride telomers, $C_nF_{2n+1}[VDF]_mI$ with m = 6 and 23. These latters were synthesized by radical telomerization of VDF with $C_nF_{2n+1}I$ initiated by bis(4-*tert*-butylcyclohexyl) peroxydicarbonate in high yields (>85%). The resulting nanohybrids were characterized by solid state NMR spectroscopy, elemental analyses and thermogravimetry. A covalent grafting between double bonds and fluorinated iodotelomers was noted. The covering density of fluorinated chains was assessed and reported with respect to fluorinated chain lengths. These nanohybrids exhibited a high thermostability (higher than 400 °C under air), losing less than 10% by weight at 700 °C, and a low surface tension, γ_s, from around 15 mN·m^{-1} to about 44 mN·m^{-1} for silica.

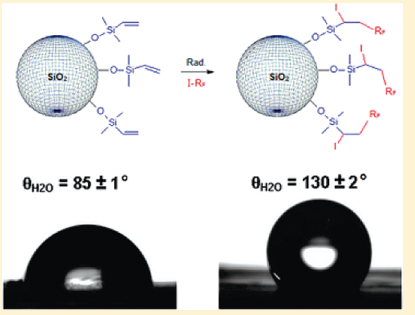

INTRODUCTION

Nanohybrids composed of an inorganic core and a polymeric shell have been of great interest to improve the properties of nanostructured materials.[1,2] In the specific case of nanocomposites, the quantity and the dispersion of nanoparticles in polymer matrix have a real impact on the properties of the final materials. Dispersion improvement generally requires a physical or chemical modification of nanoparticles surfaces.[1] Physical methods improved the physisorption of polymer chains onto particles surfaces with van der Waals interactions or Hydrogen bonds.[1] Chemical modification[3,4] or "chemisorptions" created a covalent bond between macromolecules and particles surface. Three pathways are usually considered: (i) "grafting through",[5] which generates a copolymerization between polymeric chains in growing and polymerizable groups on the surface, (ii) "grafting from",[6−16] where initiation and propagation step of polymer chains are achieved from the surface, and (iii) "grafting onto"[2,17−27] enables a covalent reaction between end-groups of polymeric chains and the surface.

The synthesis of nanocomposites combining high polarity of fillers with oleo- and hydrophoby of coating (typically fluoropolymers) is a great challenge. Additionally, it is known that these nanohybrids can be used for scratch resistant-coatings thanks to their low surface tension and high temperature.

Generally, a fluorinated silica is obtained by sol−gel process between a perfluoroalkyl di- or tri- alkoxysilane[28,29] or by condensation of perfluoroalkyl alkoxy-[30,31] (or chloro-[32,33]) silane onto silica surface or from a fluorinated functional copolymer with tetraethoxysilane and nanosilica.[34] To our knowledge, the radical addition of fluorinated chains onto silica activated with vinyl groups has never been described in the literature. Brozek and Izharov[35] reported the addition of bromine onto silica activated with vinyl groups and showed a new method to synthesize catalysts that could further be used for "grafting onto" or "grafting from" chemical modifications.

To the best of our knowledge, only Xu et al.[36] and Moody et al.[37] realized the radical addition of fluorinated mercaptans onto double bonds of polyhedral oligomeric silsesquioxane (POSS) initiated by 2,2-azobis(isobutyronitrile) (AIBN). In addition, radical additions of ω-iodoperfluorinated functional chains (tetrafluoroethylene telomers) onto unsaturated chains[38] such as allyl[39] and vinyl[40] is known to be efficient. Our approach, developed in this article, is based on these strategies[38−40] and from the procedure of Xu et al.[36] to modify the surface of silica that bears vinyl groups.

EXPERIMENTAL PART

Materials. Activated silica bearing vinyl groups (named S_{50}) with a specific area of 50 m^2/g was given from Sébastien LIVI (IMP/LMM-INSA

Received: April 21, 2011
Revised: July 11, 2011
Published: July 19, 2011

de Lyon). Perfluorohexyl iodide ($C_6F_{13}I$) and perfluorobutyl iodide (C_4F_9I) (purity 99%) were kindly supplied by Atofina (Centre de Recherche Rhône Alpes, France). These perfluoroalkyl iodides were worked up with sodium thiosulfate and then distilled prior to use to remove impurities and molecular iodine. 1,1-Difluoroethylene (vinylidene fluoride, $CH_2{=}CF_2$, VDF) was kindly supplied by Solvay S.A. (Tavaux, France). Bis(4-*tert*-butylcyclohexyl) peroxydicarbonate (BBCHPDC, Perkadox 16S) (purity 99%) and *tert*-butyl peroxypivalate (TBPPi) dissolved in isodecane (Trigonox25-C75, purity 75%) were gifts from Akzo Nobel (Chalons sur Marne, France). Sodium thiosulfate, acetonitrile (purity 99%) and deuterated acetone were purchased from Sigma-Aldrich (Saint Quentin-Fallavier, France), Riedel-de Haën (Seelze, Germany) and Euro-iso-top (Grenoble, France), respectively.

VDF telomers were synthesized by telomerization of vinylidene fluoride (VDF) with a chain transfer agent ($C_nF_{2n+1}I$ or TFE telomers) and a radical initiator, bis(4-*tert*-butylcyclohexyl) peroxydicarbonate[41] (BBCHPDC, Perkadox 16S). The radical addition of these fluorinated telomers onto silica nanoparticles was realized in acetonitrile and initiated by *tert*-butylperoxypivalate (TBPPi).

Synthesis of Vinylidene Fluoride (VDF) Telomers by Radical Telomerization. The radical telomerizations were performed in a 160 mL Hastelloy HC 276 Parr autoclave system (HC 276) equipped with a manometer, a mechanical Hastelloy anchor, a rupture disk (3000 PSI), and inlet and outlet valves. An electronic device regulated and controlled both the stirring and heating of the autoclave. Prior to reaction, the autoclave was pressurized with 30 bar of nitrogen to check for leaks. The autoclave was then conditioned for the reaction with several nitrogen/vacuum cycles (10^{-2} mbar) to remove any trace of oxygen. The liquid and dissolved solid phases (bis(4-*tert*-butylcyclohexyl) peroxydicarbonate) (7.96 g, 0.02 mol), R_F-I (13.36 or 10.38 g, 0.03 mol), and acetonitrile (80 mL)) were introduced via a funnel and then the gas (VDF) was introduced by double weighing (i.e., the difference of weight before and after filling the autoclave with the gas).

VDF (20.2 g, 0.315 mol) was added by double weighing in the reaction mixture that was progressively heated to 40, 50, or 60 °C whereupon a decrease of pressure from 19, 16, or 18 to 1 bar up was noted. This was followed by a further drop of pressure down to 0 bar in 4 h. The autoclave was then placed in an ice bath for about 60 min and was opened to yield a brown liquid. After evaporation of acetonitrile, the sample was dissolved in acetone, and the telomers produced were precipitated from methanol. The total product mixture or "crude" was filtered and the filtrate was dried by evaporation with yield higher than 90%. Hence, two fractions were obtained and noted: (1) 13.2 g of yellow powder corresponding to higher molecular weight (corresponding to 40% of total weight) and (2) 16.6 g of a brown wax as the lower molecular weight-telomer (60%). Both fractions were characterized by ^{19}F NMR spectroscopy in acetone-d_6 (Figure S1, Supporting Information).

- *Starting $C_6F_{13}I$ (Figure S1a, Supporting Information):* −65 ppm ($-CF_2\mathbf{C}F_2I$, 2F); −82 ppm ($C\mathbf{F}_3CF_2-$, 3F); −115 ppm ($-C\mathbf{F}_2-CF_2-I$, 2F); −122 ppm ($-CF_2-(C\mathbf{F}_2)_2-CF_2-CF_2-I$, 4F); −126 ppm ($CF_3-C\mathbf{F}_2-$, 2F).
- *R_F-[VDF]$_6$-I Telomer (Figure S1b, Supporting Information):* −39 ppm ($-CH_2C\mathbf{F}_2I$, 2F); absence of signals at −65 ppm; −82 ($C\mathbf{F}_3CF_2-$, 3F); −92 ppm ($-[VDF_n]-C\mathbf{F}_2CH_2$, 2*n*F) normal addition head-to-tail; −109 ppm ($-CF_2-C\mathbf{F}_2$-CH_2-I, 2F); −112 ppm ($-CF_2-CF_2-(CF_2)_x-C\mathbf{F}_2-CH_2-$) absence of signals to −113 and −116 ppm assigned to tail−tail VDF−VDF dyads; −122 to −124 ppm ($CF_3-CF_2-(C\mathbf{F}_2)_x-CF_2$, 2F); −126 ppm ($CF_3-C\mathbf{F}_2-$, 2F).

Average degree of polymerization (DP_n) values can be assessed from ^{19}F NMR spectrum (Figure S1) taking into account the integrals of signals of CF_2 assigned to VDF telomer centered at −91.0 ppm, −39.0 ppm and −109.0 ppm about that of CF_3 end group centered at −82.0 ppm (as an interesting label in ^{19}F NMR), as in eq 1[42,43]

$$\overline{DP_n} = \frac{\int \frac{CF_2^{-39ppm}}{2} + \int \frac{CF_2^{-91ppm}}{2} + \int \frac{CF_2^{-109ppm}}{2}}{\int \frac{CF_3^{-82ppm}}{3}} \quad (1)$$

where $\int CF_x^{-i\ ppm}$ represents the integral of the signal assigned to CF_x centered at $-i$ ppm.

Two VDF telomers were used in this study, $C_6F_{13}[VDF]_6I$ and $C_4F_9[VDF]_{23}I$, their ^{19}F NMR spectra are displayed in Figure S1 in the Supporting Information.

Radical Addition of TFE and VDF Telomers onto Silica-Containing Vinyl Groups. Silica activated with vinyl groups (2.00 g, referred to as S_{50} in this paper) was homogeneously dispersed into a dry acetonitrile solution (100 mL) under vigorous stirring and warmed to 74 °C. Telomer ($C_nF_{2n+1}I$ or $C_nF_{2n+1}[VDF]_mI$) and initiator (TBPPi) were added and the mixture was refluxed under stirring for 8 h, filtered and washed several times with acetone to obtain a powder. Finally, the resulting fluoro-silica was dried under vacuum (10^{-1} mmHg) at 80 °C for 8 h.

Characterization. The weight percentages of X (where X = carbon or fluorine atoms) were assessed by elemental analysis on different silica samples at the CNRS-Service Central d'Analyze (Solaize, France).

Nitrogen isotherms were achieved using a Micrometrics ASAP2020 instrument. BET (Brunauer−Emmett−Teller) theory[44] was used to determine the physical adsorption of gas molecules (nitrogen) onto silica and modified silica surface to further calculate the specific surface areas of these materials. These methods allowed calculating the tethering density (η_g) in μmol/m^2 from Berendsen:[6,15,45]

$$\eta = \frac{10^6 \times \%X}{[100M_XN_X - \%X(M_{silane} - 1)]S_{BET}} \quad (2)$$

where % X, M_X, N_X, M_{silane}, and S_{BET} represent the weight percent of X (%), the molar mass of the X atom (g mol^{-1}), the number of X atoms in the grafted silane molecule, the molar mass of the silane, and the specific surface area of the bare silica (S_{BET} = 50 m$^2\cdot$g^{-1}), respectively.

Equation 3 indicates the weight concentration (C_m in μmol$\cdot$g^{-1}) assessed from the tethering density (η) and the specific area (Sp in m$^2\cdot$g^{-1}):

$$C_m = \eta \times Sp \quad (3)$$

The Raman spectra were recorded on a LabRAM ARAMIS apparatus. A few milligrams of samples were homogeneously deposited on a glass and then irridated under a monochromatic source (473 nm). The studied wavenumber was ranging between 0 to 4000 cm^{-1}.

The X-ray powder diffraction (XRD) patterns of the products were recorded on a X'PERT PHILIPPS II diffractometer with Cu Kα radiation ($K\alpha_1$ = 1.5418 Å) at 30 kV, and Bragg angles ranged between 10 and 50°.

The liquid state NMR spectra were recorded on Bruker AC 400 instruments using deuterated acetone. Coupling constants and chemical shifts are given in hertz (Hz) and part per million (ppm), respectively. The experimental conditions for recording liquid state ^{1}H or ^{19}F NMR spectra were as follows: flip angle, 30°; acquisition time, 0.7 s; pulse delay, 2 s; number of scans, 64, and a pulse width of 5 μs.

Solid state NMR was used to qualitatively characterize the surface grafting. ^{29}Si and ^{13}C NMR spectra were recorded using cross-polarization magic angle spinning (CP-MAS) and ^{1}H one pulse (OP) on a varian VNMRS instrument (400 MHz) at 25 °C, using a 7.5 mm-diameter rotor and 3.2 mm, respectively. The experimental conditions for recording NMR spectra are listed in Table 1.

Thermogravimetry analyses were carried out on a TA Instrument Q50 apparatus. Samples were heated under a mixed atmosphere of

nitrogen and oxygen (60 and 40 mL·min^{-1}, respectively) with a ramp temperature of 20 °C/min from room temperature to 800 °C.

Surface tension was assessed from the sessile drop method used for static contact angle measurements at ambient temperature with an automatic video contact angle (CA) testing apparatus (Contact Angle System OCA-Data Physics). The probe liquids were water (θ_{H_2O}) and diiodomethane ($\theta_{CH_2I_2}$). The average CA values were determined by measuring ten different positions of the same sample with 0.8 μL and used to assess water and oil repellency of modified silica. The surface tension (γ_s) of nanoparticles were calculated with the method of Kaelble,[46,47] Owens, and Wendt[48] who used an extension of the Fowkes equation:[49]

$$\gamma_s = \gamma_s^d + \gamma_s^p \quad (4)$$

$$\sqrt{\gamma_s^d} = \frac{1 + \cos\theta_{CH_2I_2}}{2}\sqrt{\gamma_L} \quad (5)$$

$$\sqrt{\gamma_s^p} = \frac{\gamma_{LV}(1 + \cos\theta_{H_2O}) - 2\sqrt{\gamma_S^d\gamma_L^d}}{2\sqrt{\gamma_L^p}} \quad (6)$$

Here γ_s^d, γ_s^p, and γ_L or γ_{LV}, γ_L^d and γ_L^p represent the dispersive and polar components of surface tension, interfacial interactions liquid–vapor dispersive (50.8 mN·m^{-1}) and polar (72.8 mN·m^{-1}) components, and dispersive (21.8 mN·m^{-1}) and polar (51.0 mN·m^{-1}) components of water, respectively.

Table 1. Experimental Conditions Used for Recording Different Solid State Atom NMR Spectra

atom	flip angle (deg)	scans number	pulse delay (s)	frequency (kHz)
^{29}Si		1432	5	6
^{13}C		509	5	5
^{1}H	90	64	1	20

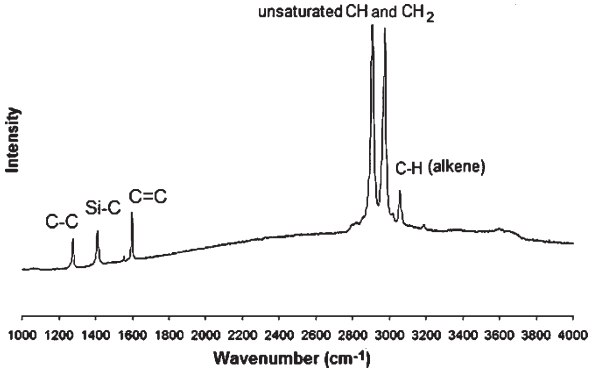

Figure 1. Raman spectrum of silica activated with vinyl groups (S_{50}).

RESULTS AND DISCUSSION

Before investigating the radical grafting of R_F-I or R_F-[VDF]$_x$-I telomers onto silica activated with vinyl groups, this functionalized silica needs to be characterized.

Characterization of Silica Bearing Vinyl Groups (S_{50}). To determine the functional groups grafted onto silica particles and the grafting efficiency of fluorinated telomers, the silica nanoparticles (S_{50}) was characterized by Raman (Figure 1), and solid state NMR spectroscopies, and by elemental analysis.

Kobler et al.[50] reported the functionalization of silica nanoparticles. This study enabled us to assign the different absorption frequencies of silica S_{50}. The vinyl groups were confirmed by the presence of vibrational bands of C–H bonds (alkene) and stretching of C=C bonds at 3070 and 1605 cm^{-1}, respectively. Other vibrational bands to 1270 cm^{-1}, 1400 cm^{-1}, 1550 and 2900 cm^{-1} were assigned to C–C, Si–C, C=C vinyl, Si–OH, and unsaturated CH and CH_2[51,52] bonds, respectively.

Nevertheless, this method did not give specific details on the structural grafting of silica activated with vinyl groups onto its

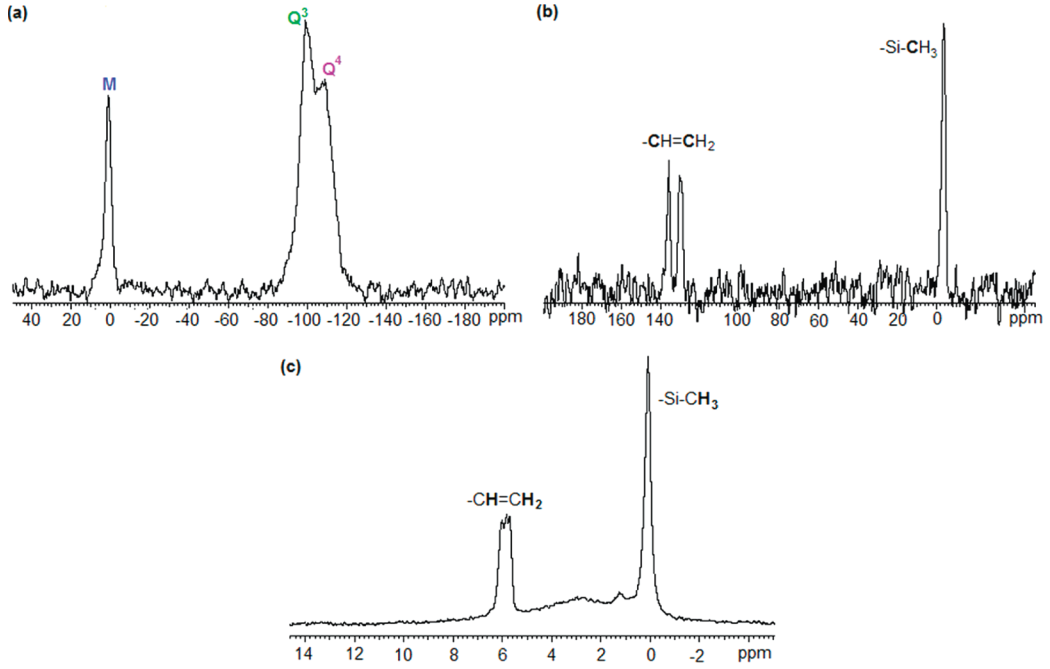

Figure 2. ^{29}Si CP-MAS (a), ^{13}C CP-MAS (b), and ^{1}H OP (c) solid state NMR spectra of silica activated with vinyl groups (S_{50}).

dx.doi.org/10.1021/ma200921b |Macromolecules 2011, 44, 6249–6257

Scheme 1. Nature of Covalent Bonds around Silicon Atoms Q^4, Q^3, or M and Corresponding Chemical Shifts at −110, −100, and 0 ppm in Solid State ^{29}Si NMR, Respectively

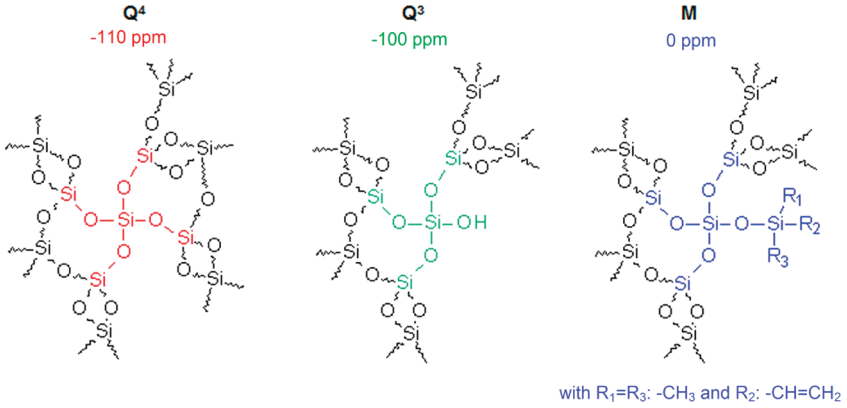

Scheme 2. Nature of Vinyl Groups onto Silica S_{50} Surface

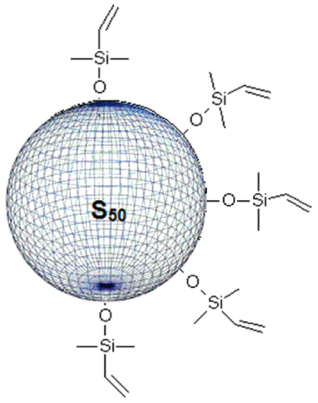

surface, and characterization by NMR solid state spectroscopy is thus required (Figure 2).

Silica particles are formed by interconnected tetrahedral SiO_4. Actually, the presence of various groups leads to strong interactions of silica with its environment.[53] Chemical shifts on ^{29}Si CP-MAS solid state NMR spectra are used to assign them. Figure 2a displays solid state NMR spectra of S_{50} silica where three chemical shifts at 0, −100, and −110 ppm are assigned to M, Q^3, and Q^4 [54−56] (Scheme 1), respectively.

Kao et al.[58] extensively reported the synthesis of functional silica with vinyl groups and their solid state NMR spectroscopy characterizations. ^{1}H NMR spectrum (Figure 2c) of the silica used in this present study shows one multiplet and one singulet centered at 6 and 0 ppm, assigned to Si−C***H***=C***H***$_2$ and Si−C***H***$_3$ groups, respectively. The decrease of the intensity of the multiplet at 6 ppm versus the fluorinated grafted chains is emphasized, because the radical grafting was carried out onto vinyl groups. Three chemical shifts observed by ^{13}C NMR spectroscopy (Figure 2b) centered at 136 ppm, 130 ppm and −4 ppm confirmed the presences of −Si−***C***H=CH$_2$, −Si−CH=***C***H$_2$, and −Si−***C***H$_3$ bonds, respectively. The proposed structure of vinyl groups grafted onto silica S_{50} surface is thus displayed in Scheme 2.

The results obtained by elemental and thermogravimetry analyses are listed in Table 3 and Figure S3 (Supporting Information). Since the functional groups grafted onto S_{50} silica surface were identified, the modification of such a vinyl silica

Table 2. Experimental Conditions Used for Grafting a Fluorinated Chain onto Silica by Radical Addition at 74 °C

silica	Sp (m^2/g)	telomers	$[R_F\text{-}I]_0$ $[-CH=CH_2]_0$	$[TBPPi]_0$ $[-CH=CH_2]_0$	N^a
S_{50}	50	C_4F_9I	15	0.05	2
		$C_6F_{13}I$			
		$C_6F_{13}[CH_2CF_2]_6I$			
		$C_4F_9[CH_2CF_2]_{23}I$			5

[a] Number of washings with acetone to obtain a constant total weight loss at 800 °C.

was carried out by radical addition of tetrafluoroethylene (TFE, C_4F_9I, and $C_6F_{13}I$) and vinylidene fluoride (VDF, C_6F_{13}-$[VDF]_6$-I and $C_4F_9[VDF]_{23}I$) telomers. In the following paragraph, the different parameters employed during the radical addition such as the reactant ratios and the length of grafted fluorinated chains are discussed.

Radical Addition of TFE and VDF Telomers onto Silica Surface. The radical addition of functional TFE or VDF telomers onto unsaturated units to modify silica nanoparticles initiated by *tert*-butylperoxypivalate (TBPPi) was inspired by previous works[38−40,57] (Scheme 3). Various C_nF_{2n+1}-$[VDF]_x$-I (where $n = 4$ or 6, and $x = 0$, 6 or 23) were used with initial $[C_nF_{2n+1}\text{-}(VDF)_x\text{-}I]_0$/[double bonds of silica]$_0$ and $[TBPPi]_0$/[double bonds of silica]$_0$ molar ratios of 15 and 0.05, respectively.

Reaction was carried out in acetonitrile at 74 °C (for which the TBPPi half-life time is 1 h) for 8 h. A high excess of fluorinated chains was added to ensure the satisfactory reactivity of all double bonds. Moreover, a blank experiment Figure S4 (Supporting Information) and Table 3, S_{50} in acetonitrile and TBPPi for 8 h) was also performed to confirm the absence of undesired reactions (that could lead to a decrease of the number of vinyl groups during the heating).

Efficient acetone washing was evidenced by thermogravimetry analysis where a constant weight loss at 800 °C (Figure S2, supporting Information) is obtained in agreement with previous results.[34]

The synthesis of silica nanoparticles that bear vinyl groups and their characterization by ^{1}H solid state NMR spectroscopy were studied by Kao et al.[58] These authors assign the signals ranging between 5.5 and 6.5 ppm to the ethylenic protons. We actually observed a decrease in their intensities revealing that the fluorinated

Table 3. Characteristics (Thermal Stabilities, Tethering Densities, Weight Concentrations, and Grafting Rates of Silica Bearing Vinyl Groups (S_{50})) and Modified by Fluorotelomers *versus* the Grafted Fluorinated Chains

			weight percentage[b] (%)		η^c (μmol·m^{-2})			
fluorinated chains grafted	total weight loss (%)	$T_d{}^a$ (°C)	C	F	C	F	$C_m{}^d$ (μmol·g^{-1})	τ^e (%)
blank	0.6	310	0.94	0	4.0	0	200	0
C_4F_9I	1	560	0.81	1.27	1.8	1.5	83	41.5
$C_6F_{13}I$	2	540	0.68	1.46	1.2	1.2	60	30.0
$C_6F_{13}[CH_2CF_2]_6I$	2	530	0.69	1.34	0.5	0.7	30	15.0
$C_4F_9[CH_2CF_2]_{23}I$	8	500	4.13	5.86	1.5	1.3	70	35.0

[a] Decomposition temperature of grafted chains determined from the derivative of TGA thermograms (Figure S3, Supporting Information). [b] % X: weight percentage of atoms X (assessed by elemental analysis). [c] η(X): tethering density (μmol.m^{-2}) of silanes calculated from eq 1. [d] Weight concentration assessed from eq 2. [e] Grafting rate assessed from eq 7.

Scheme 3. Radical Addition of ω-Iodofluorinated Chains (R_F-I) onto Double Bonds at the Surface of Silica

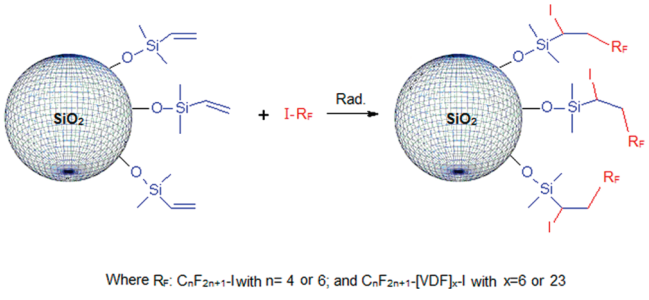

Where R_F: C_nF_{2n+1}-I with n= 4 or 6; and C_nF_{2n+1}-[VDF]$_x$-I with x=6 or 23

chains are grafted onto particles surface, as shown in Figure 3. This figure displays the 4−8 ppm range of ^{1}H solid state NMR spectra where the difference is clearly observed for the signals intensities between those assigned to the vinyl groups stemming from both silica (lower spectrum) and modified fluorinated chains (four other spectra) as the chain length varied.

To confirm the efficient grafting of VDF and TFE telomers onto silica, complementary characterizations were performed such as elemental analyses, thermogravimetry, and water and diiodomethane contact angle measurements to assess the surface tension.

Evaluation of the efficiency of TFE ($C_nF_{2n+1}I$) and VDF ($C_nF_{2n+1}[VDF]_mI$) telomers grafting. The tethering (η, eq 2) and the weight concentration (C_m, eq 3) were assessed to quantify the total amount of telomers present at the surface. The results of elemental analysis from modified silica (in weight percents of the studied atoms such as carbon and fluorine) are displayed in Table 3.

Thermogravimetry analyses (under air) were carried out to determine the weight amount of fluorinated chains grafted on the silica surface. Figure 4 shows the weight evolution versus temperature. The total weight loss of silica and grafted silica at 800 °C are listed in Table 3.

Silica nanoparticles modified with TFE telomers and C_6F_{13}-[VDF]$_6$I show onset temperatures of ca. 450 °C. However, silica modified by $C_4F_9[VDF]_{23}I$ displays two weight losses (at 200 and 450 °C) assigned to physisorbed and chemisorbed chains, respectively. Indeed, the physisorbed $C_4F_9[VDF]_{23}I$ chains were not completely eliminated during the process of acetone washing (Figure 4). The interaction nature between this telomer chain and silica surface is discussed hereafter.

A good agreement was observed between the tethering densities (η) calculated from weight percentages of carbon and

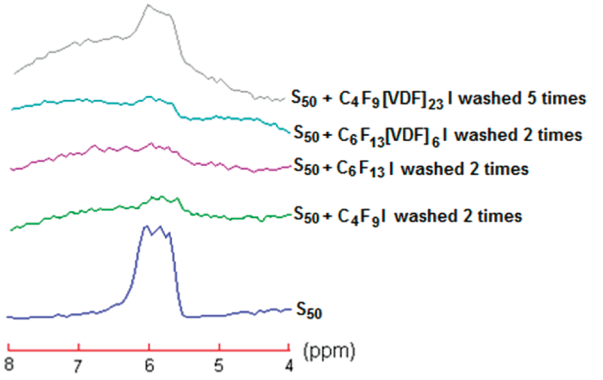

Figure 3. Expansion of the 4−8 ppm zone of the ^{1}H one pulse (OP) solid state NMR spectra of silica activated with vinyl groups (S_{50}, bottom) and the same silica modified with TFE telomers C_4F_9I (above bottom) and $C_6F_{13}I$ (middle), and VDF telomers $C_6F_{13}[VDF]_6I$ (second spectrum from top) and $C_4F_9[VDF]_{23}I$ (upper spectrum).

fluorine atoms (eq 2). The weight concentration of vinyl groups at the silica S_{50} (200 μmol.g^{-1}) surface decreased versus the length of grafted fluorinated chains (83 μeq·g^{-1} for C_4F_9I). Indeed, silica modified with VDF telomers (DP_n = 23) presents a weight concentration (70 μmol·g^{-1}) higher than that of silica modified with a short chain (e.g., 30 μmol·g^{-1} for a telomer of DP_n = 6). Such a behavior arises from the long chain physisorption of these fluorinated telomers that contain a high amount of VDF units.

The evolution of the surface tension of fluorinated silica was studied by the assessment of contact angle with sessile drop method (Figure 5) of polar (water) and apolar (diiodomethane) solvents. Averaged contact angle values and resulting surface tension are listed in Table 4.

As shown in Figure 5, the water contact angles (WCAs) and diiodomethane contact angles (DICAs) exhibit a great increase ranging from WCA= 85 ± 1° and DICA= 34 ± 1° for S_{50} silica to WCA= 140 ± 1°or 130 ± 2° and DICA= 88 ± 5° or 86 ± 4° for silica modified by $C_6F_{13}I$ and VDF telomers, respectively. The grafting of fluorinated telomers onto silica nanoparticles thus clearly favors an increase in the hydro- and oleophoby of such a silica (Table 4).

Hence, grafting silica with TFE telomers increased the surface hydrophoby compared to that achieved from VDF telomers. This behavior certainly arises from the presence of hydrogen atoms in VDF units[56,57] (Scheme 4), and confirm Shafrin and Zisman's[59] and Pitman's[60] theories.

dx.doi.org/10.1021/ma200921b |*Macromolecules* 2011, 44, 6249–6257

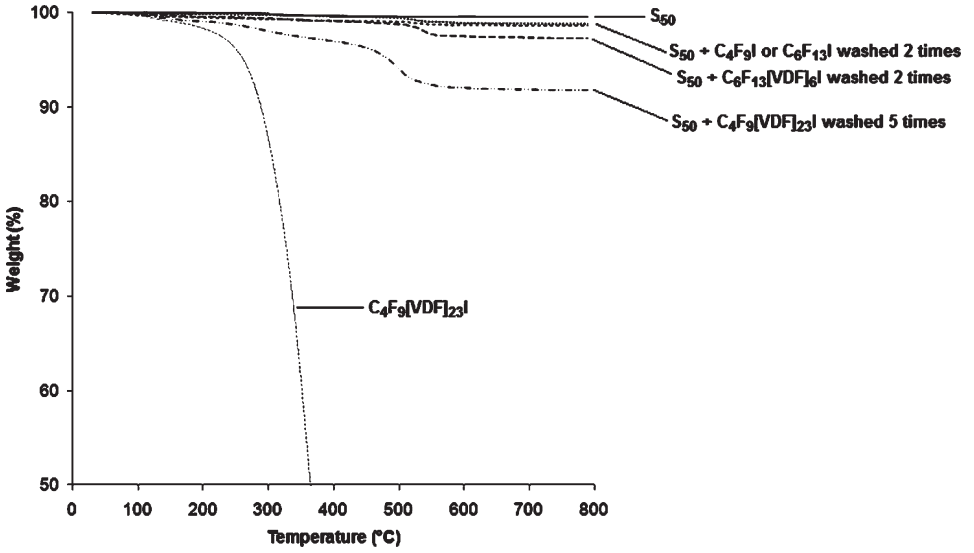

Figure 4. TGA thermograms under air of $C_4F_9[VDF]_{23}I$ and silica bearing vinyl groups (S_{50}) and modified by TFE (C_4F_9I and $C_6F_{13}I$) or VDF ($C_6F_{13}[VDF]_6I$ and $C_4F_9[VDF]_{23}I$) telomers, after various washings.

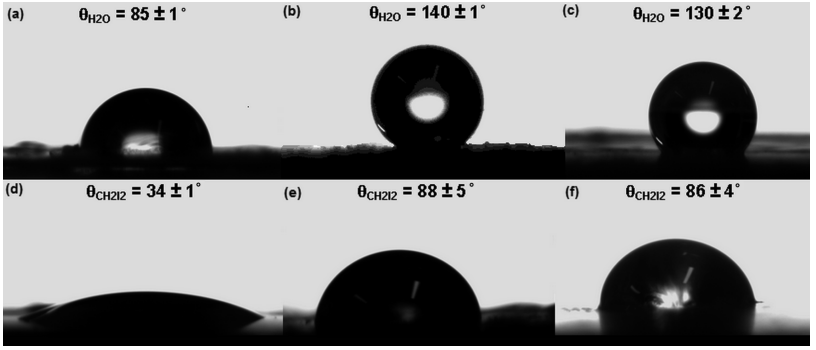

Figure 5. Pictures of water and diiodomethane droplets on silica that bears vinyl groups (a and d) or modified with $C_6F_{13}I$ (b and e) and $C_4F_9(VDF)_{23}I$ (c and f) telomers.

Table 4. Water and Diiodomethane Contact Angles Values and Surface Tensions for Silica That Bears Vinyl Groups and Modified with TFE and VDF Telomers

		contact angle[a](deg)				
silica	fluorinated chain	θ_{WCA}	θ_{DICA}	γ_s^{db} (mN m^{-1})	γ_s^{pb} (mN m^{-1})	$\gamma_s{}^b$ (mN m^{-1})
S_{50}	none	85 ± 1	34 ± 1	42.4	1.4	43.8
	C_4F_9I	125 ± 2	52 ± 2	20.4	0.6	21.0
	$C_6F_{13}I$	140 ± 1	88 ± 5	13.5	1.5	15.5
	$C_6F_{13}[CH_2CF_2]_6I$	121 ± 1	55 ± 3	19.9	0.2	20.1
	$C_4F_9[CH_2CF_2]_{23}I$	130 ± 2	86 ± 4	14.5	0.8	15.3

[a] θ_{H_2O} and $\theta_{CH_2I_2}$: averaged experimental values of contact angle measurements assessed by sessile drop method (pictures of water and diiodomethane drop on bare and grafted silicas in Figure 5) . [b] $\gamma_s{}^d$ and $\gamma_s{}^p$ represent the dispersive (eq 5 in experimental part) and polar (eq 6) components of surface tension, respectively, while γ_S stands for the surface tension (eq 4).

Physisorption of VDF Telomers. Despite a great care in acetone washings, elemental and thermogravimetry analyses (Table 3) have shown the presence of physisorbed $C_4F_9[VDF]_{23}I$ telomers. Such an occurrence is actually explained by the length of telomer grafting onto silica surface. A previous work[41] has shown the dependence of the crystallinity of these telomers versus the number of VDF units. Indeed, the telomers with a degree of polymerization (DP_n) of 19 exhibit a high crystallinity rate (ca. 80%). This value has to be put in contrast with the one obtained for telomers with 6 VDF units, the behavior of which is organic-like molecule, i.e. no entanglement of chains, and the formation of a crystal lattice.

XRD patterns (Figure 6) of (i) silica that bears vinyl groups (S_{50}) and (ii) modified silica with $C_4F_9[VDF]_{23}I$ telomer were

Scheme 4. Evolution of the Surface Tension *versus* Fluorinated Chains Grafted onto Silica Nanoparticles

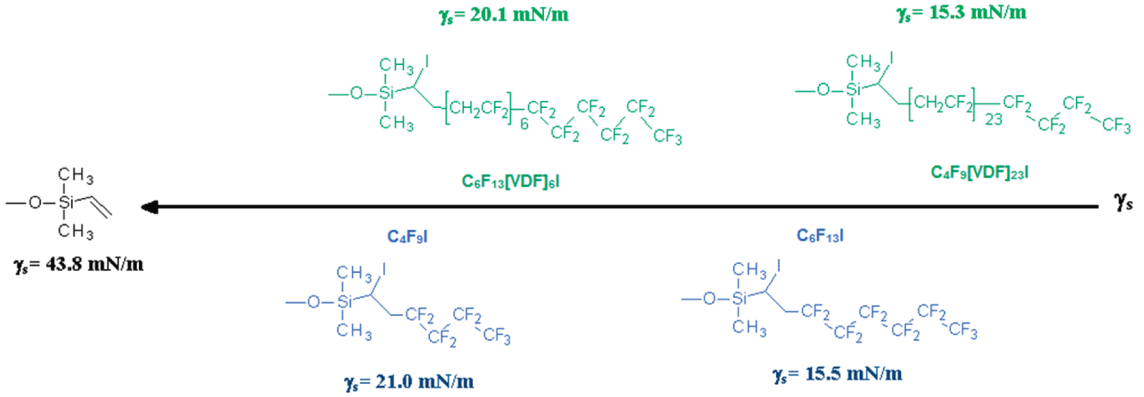

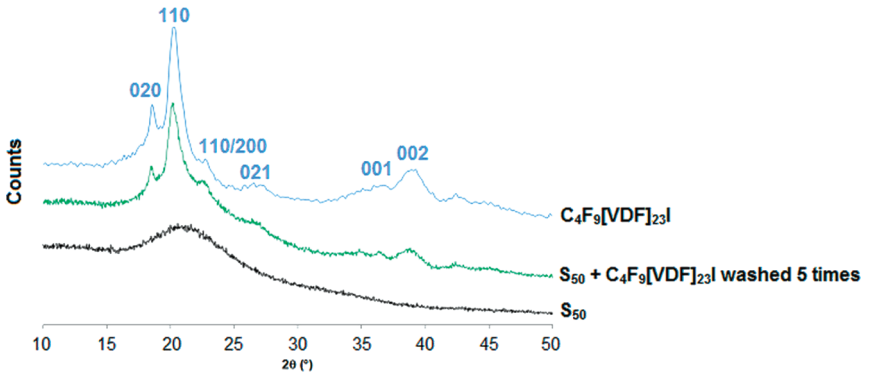

Figure 6. X-ray diffraction patterns of S_{50} vinyl silica (lowest spectrum), of $C_4F_9[VDF]_{23}I$ (uppest spectrum) telomers only, and of silica modified with the same telomer (middle spectrum).

Scheme 5. Sketch of the Efficiency of the Radical Additions of TFE (C_4F_9I or $C_6F_{13}I$) or VDF ($C_6F_{13}[VDF]_6I$) Telomers with Respect to the Lengths of Telomers onto Silica That Bears Vinyl Groups (S_{50})

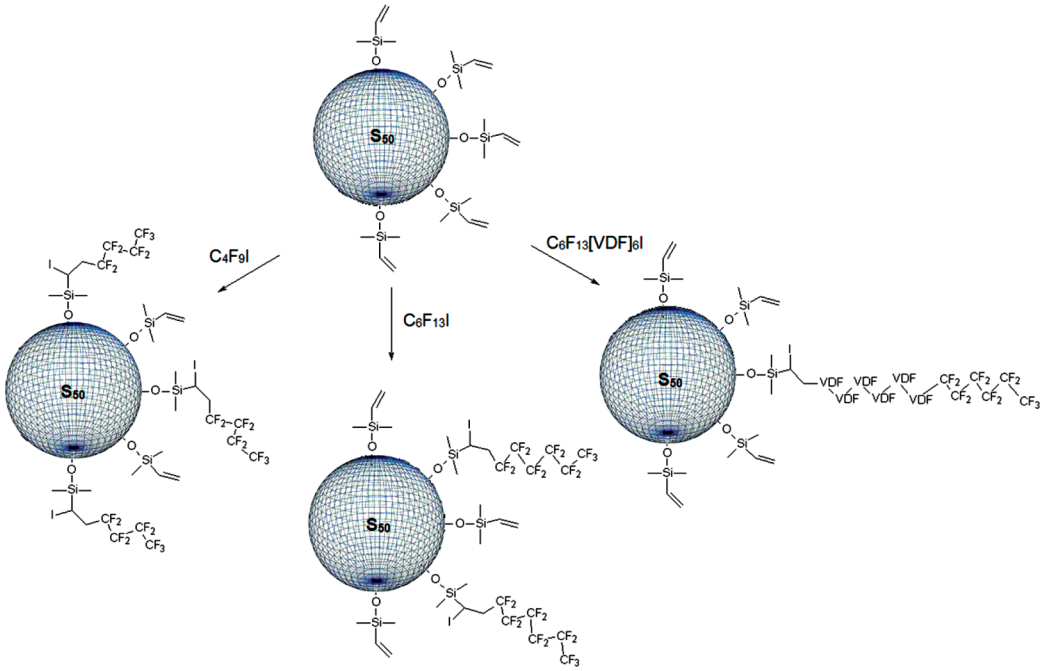

dx.doi.org/10.1021/ma200921b |*Macromolecules* 2011, 44, 6249–6257

compared. The presence of fluorinated crystallized chains onto the silica surface was thus confirmed.

From Imran-ul-Haq et al.[61] and Elashawi and Hakeem's[62] works, XRD patterns reveal the coexistence of two crystalline forms (α and β) of VDF telomers. Diffraction peaks located at 2θ (plan) of 17.70° (100), 18.42° (020), 20.12° (110), 26.70° (021), and 38.68° (002) have been attributed to the α crystal. The other peaks, centered at 22.70° (110/200) and 36.45° (001), have been assigned to the β form.[41] The presence of crystalline plans onto silica modified surface explained the physisorption phenomenon.

Decreasing of the Tethering Density versus the Chain Length. Table 3 compares the weight concentration (C_m) versus fluorinated telomers grafted onto nanoparticles surface. The calculation of weight concentration in vinyl groups of silica S_{50} (200 μmol/g, assessed from eqs 2 and 3) evidence a decrease in these unsaturations after the radical addition of fluorinated telomers. The concentration in fluorinated chains based on both TFE (C_4F_9I or $C_6F_{13}I$) and VDF telomers, with a DP_n of 6 (that does not exhibit any crystal forms) at the surface of silica showed a decrease to 83, 60, and 30 μmol·g^{-1}, respectively. Such a behavior is explained by steric hindrance of fluorinated chains grafted onto the silica surface (Scheme 5).

From weight concentrations (Table 3) of vinyl groups onto silica surface, S_{50} (200 μmol.g^{-1}), and vinyl groups which reacted with fluorinated telomers, it was thus possible to determine a grafting rate of fluorinated chains from eq 7:

$$\tau = \frac{C_{m\mathrm{RF}}}{C_m} \times 100 \qquad (7)$$

where τ, $C_{m\mathrm{RF}}$ and C_m stand for the grafting rate of fluorinated chains onto the particle surface (%), the weight concentration of telomers ($-Si(CH_3)_2-CHI-CH_2-R_F$) in μmol·g^{-1}) and the massic concentration of vinyl groups onto silica surface (200 μmol·g^{-1}), respectively. The resulting grafting rate decreases with the chain length, in very good agreement with that shown above on the surface modification.

Nevertheless, the assessment of the surface tensions (eq 4 to 6) of these fluorinated particles from contact angles determined by the sessile drop method of polar (water) and apolar (diiodomethane) solvents confirms the influence of both (i) the chain length for the same series of fluorotelomer and (ii) the presence of hydrogen atoms in the VDF telomers. Indeed, surface tension of silica modified with C_4F_9I and $C_6F_{13}I$ varied from 21.0 to 15.5 mN·m^{-1}, respectively and when hydrogen atoms were inserted as in the case of VDF telomers (e.g., $C_6F_{13}[VDF]_6I$), the value increased to 20.1 mN·m^{-1}.

CONCLUSIONS

The modification of vinyl silica by radical addition of tetrafluoroethylene (TFE, $C_nF_{2n+1}I$ where n = 4 or 6) or vinylidene fluoride (VDF, $C_nF_{2n+1}[VDF]_mI$ where m = 6 or 23) telomers was initiated by *tert*-butylperoxypivalate at 74 °C. Such a simple reaction led to very good yields. Washing these modified silica with acetone was necessary, as evidenced by thermogravimetry analysis. In case of crystalline VDF telomers, the physisorbed chains remained, despite washing. It was argued that important interactions between chains (like physical knots) exist, and they lead to chains crystallization onto the silica surface. The reactivity of vinyl groups toward the fluorinated telomer was monitored by ^{1}H OP NMR spectroscopy. Thermogravimetry analysis, as well as elemental analysis confirmed the effect of chain length on the covering density. Indeed, the covering density of modified silica is in agreement with the influence of the chain length linked to the steric effect and physisorption of long chains ($C_4F_9[VDF]_{23}I$). Physisorption phenomenon and entanglement are actually limited by a decrease in VDF units inside the telomers ($C_6F_{13}[VDF]_6I$ or TFE telomers). Finally, the contact angle measurement indicated the sharp evolution of hydro- and oleophoby of these original fluorosilica. Initial vinyl silica exhibited a surface tension of 43.8 mN·m^{-1} which is clearly higher than that assessed after the modification with fluorinated telomers, that was as low as 15 mN·m^{-1}.

ASSOCIATED CONTENT

Supporting Information. ^{19}F NMR spectra of $C_6F_{13}I$ and $C_6F_{13}(VDF)_6I$, TGA thermograms (under air) and their derivatives of silica that bears vinyl groups and modified by $C_4F_9(VDF)_{23}I$ versus the number of acetone washings, and ^{1}H NMR spectra of silica S50 and a blank. This material is available free of charge via the Internet at http://pubs.acs.org/.

AUTHOR INFORMATION

Corresponding Author
*E-mail: bruno.ameduri@enscm.fr. Fax: (+33) 467-147-720.

ACKNOWLEDGMENT

The authors thank the National Agency of Research (NaFEL project from ANR "Matériaux & Procédés") for financial support, J.-F. Gérard, J. Duchet and S. Livi (INSA Lyon) to offer silica activated with vinyl groups (S_{50}), and D. Bourgogne and D. Granier from University of Montpellier II who recorded Raman spectra and X-ray diffraction patterns, respectively.

REFERENCES

(1) Zou, H.; Wu, S.; Shen, J. *Chem. Rev.* **2008**, *108*, 3893–3957.
(2) Achilleos, S. D.; Vamvakaki, M. *Materials* **2010**, *3*, 1981–2026.
(3) Ruiz-Hitzky, E. *Chem. Rec.* **2003**, *3*, 88–100.
(4) Hoffmann, F.; Cornelius, M.; Morell, J.; Fröba, M. *Angew Chem. Int. Ed.* **2006**, *45*, 3216–3251.
(5) Wang, Y.; Ke, Y.; Li, J.; Du, S.; Xia, Y. *China Particuology* **2007**, *5*, 300–304.
(6) (a) Flesh, C.; Delaite, C.; Dumas, P.; Bourgeat-Lami, E.; Duguet, E. *J. Polym. Sci., Part A: Polym. Chem.* **2004**, *42*, 6011–6020. (b) Joubert, M.; Delaite, C.; Bourgeat-Lami, E.; Dumas, P. *Macromol. Rapid Commun.* **2005**, *26*, 602–607. (c) Bartholome, C.; Beyou, E.; Bourgeat-Lami, E.; Chaumont, P.; Lefebvre, F.; Zydowicz, N. *Macromolecules* **2005**, *38*, 1099–1106. (d) Konn, C.; Morel, F.; Beyou, E.; Chaumont, P.; Bourgeat-Lami, E. *Macromolecules* **2007**, *40*, 7464–7472.
(7) Barbey, R.; Lavanant, L.; Paripovic, D.; Schüwer, N.; Sugnaux, C.; Tugulu, S.; Klok, H. A. *Chem. Rev.* **2009**, *109*, 5437–5527.
(8) Radhakrishnan, B.; Ranjan, R.; Brittain, W. J. *Soft Matter* **2006**, *2*, 386–396.
(9) Perruchot, C.; Khan, M. A.; Armes, S. P. *Langmuir* **2001**, *17*, 4479–4481.
(10) Li, X.; Hong, C. Y.; Pan, C. Y. *Polymer* **2010**, *51*, 92–99.
(11) Carrot, G.; Diamanti, S.; Manuszak, B.; Charleux, B.; Vairon, J. P. G. *J. Polym. Sci., Part A: Polym. Chem.* **2001**, *39*, 4294–4301.
(12) El Harrak, A.; Carrot, G.; Oberdisse, J.; Eychenne-Baron, C.; Boue, F. *Macromolecules* **2004**, *37*, 6376–6384.
(13) El Harrak, A.; Carrot, G.; Oberdisse, J.; Jestin, J.; Boue, F. *Polymer* **2005**, *46*, 1095–1104.

(14) Save, M.; Granvorka, G.; Bernard, J.; Charleux, B.; Boissière, C.; Grosso, D.; Sanchez, C. *Macromol. Rapid Commun.* **2006**, *27*, 393–398.
(15) (a) Pardal, F.; Lapinte, V.; Robin, J. J. *J. Polym. Sci., Part A: Polym. Chem.* **2009**, *47*, 4617–4628. (b) Yu, H.-J.; Luo, Z.-H. *J. Polym. Sci., Part A: Polym. Chem.* **2010**, *48*, 5570–5580.
(16) Liberelle, B.; Giasson, S. *Langmuir* **2007**, *23*, 9263–9270.
(17) Impens, N. R. E. N.; Van der Voort, P.; Vansant, E. F. *Microporous Mesoporous Mater.* **1999**, *28*, 217–232.
(18) Suzuki, K.; Siddiqui, S.; Chappell, C.; Siddiqui, J. A.; Ottenbrite, R. M. *Polym. Adv. Technol.* **2000**, *11*, 92–97.
(19) Spange, S. *Prog. Polym. Sci.* **2000**, *25*, 781–849.
(20) Carrot, G.; Rutot-Houzé, D.; Poitier, A.; Degée, P.; Hilborn, J.; Dubois, P. *Macromolecules* **2002**, *35*, 8400–8404.
(21) Dyer, J. D. *Adv. Polym. Sci.* **2006**, *197*, 47–65.
(22) Bachmann, S.; Wang, H.; Albert, K.; Partch, R. J. *Colloid Interface Sci.* **2007**, *309*, 169–175.
(23) Cai, L. F.; Mai, Y. L.; Rong, M. Z.; Ruan, W. H.; Zhang, M. Q. *Express Polym. Lett.* **2007**, *1*, 2–7.
(24) Gann, J. P.; Yan, M. *Langmuir* **2008**, *24*, 5319–5323.
(25) Kar, M.; Vijayakumar, P. S.; Prasad, B. L. V.; Gupta, S. S. *Langmuir* **2010**, *26*, 5772–5781.
(26) Yu, Y.; Rong, M. Z.; Zhang, M. Q. *Polymer* **2010**, *51*, 492–499.
(27) (a) Hübner, H.; Allgaier, J.; Meyer, M.; Stellbrink, J.; Pyckhout-Hintzen, W.; Richter, D. *Macromolecules* **2010**, *43*, 856–867. (b) Durand, N.; Mariot, D.; Ameduri, B.; Boutevin, B.; Ganachaud, F. *Langmuir* **2011**, *27*, 4057–4067.
(28) Sawada, H.; Sasaki, A.; Sasazawa, K.; Toriba, K. I.; Kakehi, K. I.; Miura, M. *Polym. Adv. Technol.* **2008**, *1*, 76371–76380.
(29) Matsuo, Y.; Yamada, Y.; Nishikawa, M.; Fukutsuka, T.; Sugie, Y. *J. Fluorine Chem.* **2008**, *129*, 1150–1155.
(30) Sheen, Y. C.; Huang, Y. C.; Liao, C. S.; Chou, H. Y.; Chang, F. C. *J. Polym. Sci., Part B: Polym. Phys.* **2008**, *46*, 1984–1990.
(31) Hongxia Wang, H.; Fang, F.; Cheng, T.; Ding, J.; Qu, L.; Dai, L.; Wang, X.; Lin, T. *Chem. Commun.* **2008**, *7*, 877–879.
(32) Ogawa, M.; Miyoshi, M.; Kuroda, K. *Chem. Mater.* **1998**, *10*, 3787–3789.
(33) Tarasevich, Y. I.; Polyakov, V. E.; Serdan, A. A.; Lisichkin, G. V. *Colloid J.* **2004**, *66*, 592–597.
(34) Sawada, H.; Tashima, T.; Nishiyama, Y.; Kikuchi, M.; Goto, Y.; Kostov, G.; Améduri, B. *Macromolecules* **2011**, *44*, 1114–1124.
(35) Brozek, E. M.; Izharov, I. *Chem. Mater.* **2009**, *21*, 1451–1456.
(36) Xu, J.; Li, X.; Cho, C. M.; Toh, C. L.; Shen, L.; Mya, K. Y.; Lu, X.; He, C. *J. Mater. Chem.* **2009**, *19*, 4740–4745.
(37) Moody, L. E.; Marchant, D.; Grabow, W. W.; Lee, A. Y.; Mabry, J. M. Presented at the SAMPE 2005 Fall Technical Conference (37th ISSE), Seattle, WA, 31 Oct−3 Nov 2005.
(38) Améduri, B.; Boutevin, B.; Nouiri, M.; Talbi, M. *J. Fluorine Chem.* **1995**, *74*, 191–197.
(39) Manséri, A.; Améduri, B.; Boutevin, B.; Kotora, M.; Hajek, M.; Caporiccio, G. *J. Fluorine Chem.* **1995**, *73*, 151–158.
(40) Balagué, J.; Améduri, B.; Boutevin, B.; Caporiccio, G. *J. Fluorine Chem.* **2000**, *102*, 258–265.
(41) Durand, N.; Ameduri, B.; Boutevin, B. *J. Polym. Sci., Part A: Polym. Chem.* **2011**, *49*, 82–92.
(42) Boyer, C.; Valade, D.; Sauguet, L.; Ameduri, B.; Boutevin, B. *Macromolecules* **2005**, *28*, 10353–10362.
(43) Boyer, C.; Valade, D.; Lacroix-Desmazes, P.; Ameduri, B.; Boutevin, B. *J. Polym. Sci. Part A: Polym Chem* **2006**, *44*, 5763–5777.
(44) Brunauer, S.; Emmett, P. H.; Teller, E. *J. Am. Chem. Soc.* **1938**, *60*, 309–319.
(45) Bourgeat-Lami, E.; Espiard, Ph.; Guyot, A. *Polymer* **1995**, *36*, 4385–4389.
(46) Kaelble, D. H.; Uy, K. C. *J. Adhes.* **1970**, *2*, 50–60.
(47) Kaelble, D. H. *J. Adhes.* **1970**, *2*, 66–81.
(48) Owens, D. K.; Wendt, R. C. *J. Appl. Polym. Sci.* **1969**, *13*, 1741–1747.
(49) Fowkes, F. H. *Adv. Chem. Ser.* **1964**, *43*, 99–111.
(50) Kobler, J.; Möller, K.; Bein, T. *ACS Nano* **2008**, *2*, 791–799.
(51) Niepceron, F.; Laffite, B.; Galiano, H.; Bigarre, J.; Nicol, E.; Tassin, J.-F. *J. Membr. Sci.* **2009**, *338*, 100–110.
(52) Carmano-Quiroga, P. M.; Martinez-Ramirez, S.; Blanco-Varela, Y. M. T. *Mater. Construccion* **2008**, *58*, 233–246.
(53) Zhurodlev, L. T. *Colloids Surf. A: Phys. Chem. Eng. Aspects* **2000**, *173*, 1–38.
(54) (a) Mercier, L.; Pinnavaia, T. J. *Adv. Mater.* **1997**, *9*, 500–503. (b) Zhao, X. S.; Lu, G. Q. *J. Phys. Chem. B* **1998**, *102*, 1556–1561.
(55) Bourgeat-Lami, E.; Lang, J. *J. Colloid Interface Sci.* **1998**, *197*, 293–308.
(56) Sutra, P.; Fajula, F.; Brunel, D.; Lentz, P.; Daelen, G.; Nagy, J. B. *Coll. Surf. A* **1999**, *158*, 21–27.
(57) Nouiri, M.; Ameduri, B.; Boutevin, B. *J. Polym. Sci. Part A; Polym. Chem.* **1993**, *31*, 2069–2080.
(58) Kao, H. M.; Chang, P. C.; Wu, J. D.; Chiang, A. S. T.; Lee, C. H. *Microporous Mesoporous Mat.* **2006**, *97*, 9–20.
(59) Shafrin, E. G.; Zisman, W. A. *J. Phys. Chem.* **1960**, *64*, 519–524.
(60) Pittman, A. G. *Surface properties of fluorocarbon polymers in high polymers*; Wiley: New-York, 1972, 25, 419−449.
(61) Imran-ul-Haq, M.; Tiersch, B.; Beuermann, S. *Macromolecules* **2008**, *41*, 7453–7462.
(62) Elashmawi, I. S.; Hakeem, N. A. *Polym. Eng. Sci.* **2008**, *48*, 896–901.